HE 2.3.02

Muon Component in Giant Air Showers with Energy of $\geq 10^{19}$eV Observed by AGASA

AGASA Collaboration
presented by N.Inoue

Department of Physics, Saitama University, Urawa 338-8570, Japan

Abstract

The chemical composition of cosmic rays in the ultra-high energy region of $10^{18.5}$eV – $10^{20.5}$eV has been studied with muon component in air showers observed by the AGASA of 100km^2 area (A100). The relation among the muon density at 1000m from the core ($\rho_\mu(1000)$), the charged particle density at 1000m ($S(1000)$) and primary energy (E_0) is compared with simulation results. $\rho_\mu(1000)$ in the highest energy region ($> 10^{19}$eV) can be explained by the nucleonic showers and there is no candidate shower of gamma-ray primary.

1 Introduction

The chemical composition of cosmic rays with energy greater than $10^{17.0}$eV is still unsolved. The Fly's Eye group has studied it from the energy dependence of the depth at shower maximum(X_{max}) above 10^{17}eV (Bird et al., 1993) and reported that composition around $(1-3) \times 10^{17}$eV is predominantly heavy, however, it becomes gradually lighter above 3×10^{17}eV and becomes predominantly proton around 10^{19}eV. At Akeno the composition study has been made from the analysis of muon component for showers with energies greater than 10^{16}eV (Hayashida et al.,1995,1997). From this analysis, no indication in the significant change of the primary composition around 3×10^{17}eV has been found, since $\rho_\mu(600)$ increases with $S(600)$ smoothly without any change of slope around 3×10^{17}eV. In the highest energy region($E_0 \geq 10^{19}$eV), various models have been proposed as cosmic ray origin: active astrophysical object(ex., Rachen and Biermann, 1993), decay products of much higher energy particles such as superheavy relic particles (ex, Berezinsky et al.,1997) or topological defects(ex., Bhattacharjee et al., 1992), and have predicted the presence of gamma-ray primaries in the highest energy region, whose flux depends much on the models on their production or propagation in the intergalactic space.

According to the Monte Carlo simulation, the local muon density at 1000m (ρ_μ (1000)) in showers initiated by heavy primaries is expected to be larger than that by light composition at the same primary energies. If significant change of chemical composition occurs in some energy, the rate of change of $\rho_\mu(1000)$ with energy may be observed in that energy.

In case of gamma-ray primaries, two effects must be taken into account. One is the Landau-Pomeranchuk-Migdal (LPM) effect (Landau and Pomeranchuk, 1953; Migdal, 1956) and the other is electron-positron pair creation in the geomagnetic field (McBreen and Lambert, 1981). Since the primary energy of the present experiment is estimated from $S(600)$, the energies from gamma-ray primary showers are in some cases underestimated due to the LPM effect. However, if their arrival direction is nearly perpendicular to the geomagnetic field lines, their energy may not be reduced, since the showers are a bunch of electromagnetic cascades of lower energies. Therefore there is a possibility that a low $\rho_\mu(1000)$ showers are found in the giant air showers, if there are gamma-rays in the highest energy cosmic rays, depending on their arrival directions.

2 Experiment and Results

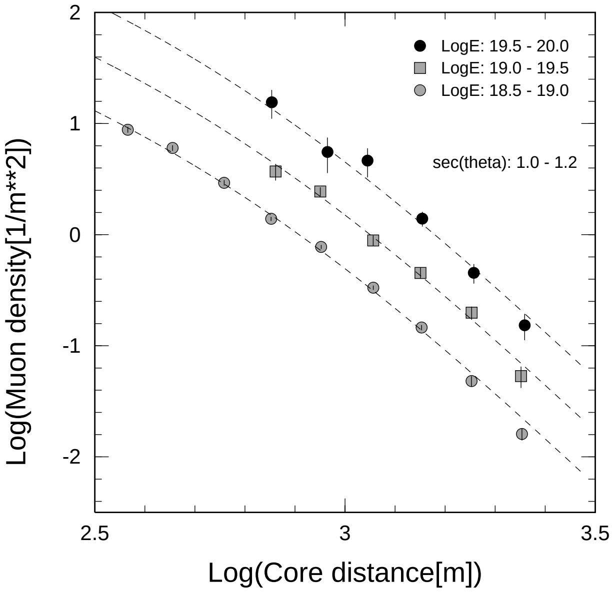

Figure 1: *The lateral distributions of muons ($E_\mu \geq 0.5sec\theta$ GeV) in air showers with energies of $10^{18.75}$eV, $10^{19.25}$eV and $10^{19.75}$eV are plotted. Showers with sec $\theta \leq 1.2$ and . Broken lines show the experimental lateral distribution function of muons described in the text.*

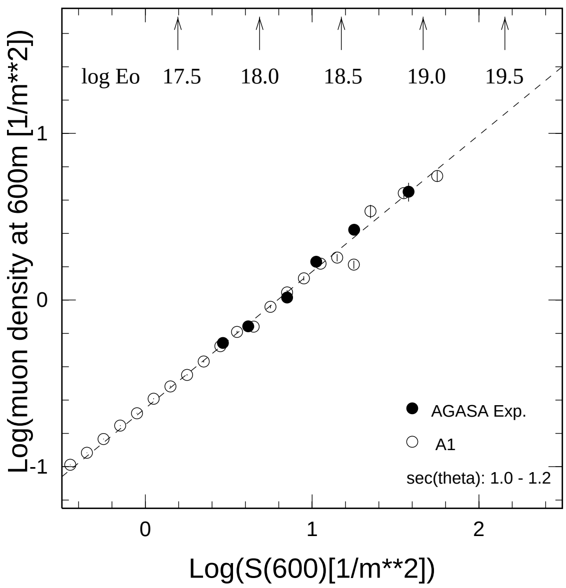

Figure 2: *The relation between ρ_μ(600) and S(600) for showers with $sec\theta \leq 1.2$. Results of present analysis from A100 is shown with closed circles. Result and the corrlation from A1 are shown with open circles and broken line, respectively.*

Details of the experiments are described in Chiba et al.(1992) and Ohoka et al.(1997).Present analysis of muon component(threshold energy:$E_\mu \geq 0.5 \times \sec\theta$ GeV) has been made with data taken by 15 detectors in SUDAMA Branch and 12 detectors in AKENO Branch since September 1993. The number of events with $\sec\theta \leq 1.2$ used in the present analysis is 69,999 up to March 1999.

The lateral distributions of muon for showers with energies of $10^{18.75}$eV, $10^{19.25}$eV and $10^{19.75}$eV and $\sec\theta \leq 1.2$ (1.09 in average) are shown in Figure 1. Its empirical formula determined in this analysis is expressed as below and is shown with broken lines in the figure.

$$\rho_\mu(R) = N_\mu(C_\mu/{R_0}^2)(R/R_0)^{-0.75}(1+R/R_0)^{-2.52}(1+(R/800\text{m})^2)^{-0.6}$$

where R is the distance from the core, N_μ is the total number of muons, and C_μ is a normalization factor. R_0 is a characteristic distance (277m for $\sec\theta = 1.09$).

Shape of muon lateral distributions in the energy between $10^{18.5}$eV and $10^{20.0}$eV is almost consistent with that expected from the formula determined for showers with lower energy region in a core distance region of 800m – 2000m. Energy dependence of slope in lateral distribution between 800m – 2000m is not found beyond the experimental error even for nearly up to 10^{20}eV. $\rho_\mu(600)$ and $\rho_\mu(1000)$ are derived from observed muon densities at 500m – 800m and 800m – 1580m, respectively, and they are normalized to that at 600m and 1000m using the lateral distribution function mentioned above. In Figure 2, the relation between $\rho_\mu(600)$ and $S(600)$ for showers with $\sec\theta \leq 1.2$ and energies of $10^{17.5}$eV – $10^{19.0}$eV is shown and the result from Akeno 1km^2 array (A1) with threshold energy of $E_\mu \geq 1.0 \times \sec\theta$ GeV is also shown with open circles. In this figure, $\rho_\mu(600)$ from A1 is enhanced by

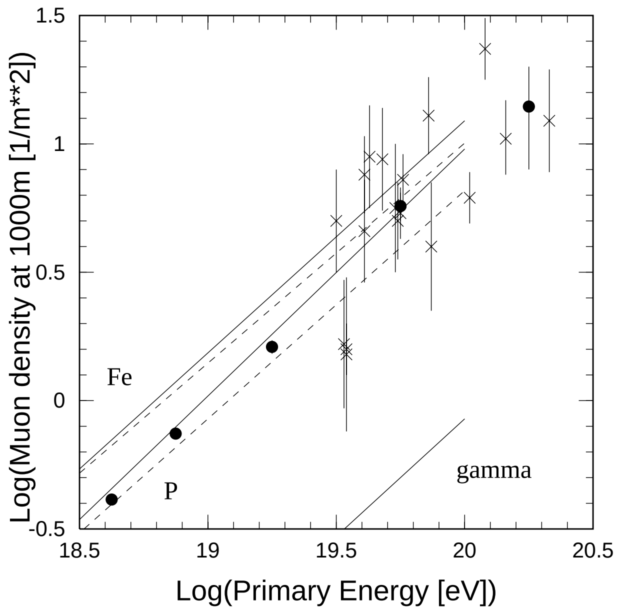

Figure 3: *The relation between ρ_μ(1000) and E_0 for showers with secθ $\leq$ 1.2. Results of CORSIKA-QGSJET simulation are shown with solid lines for proton, iron and gamma-ray primaries. Simulation results by Dedenko are shown with broken lines for proton and iron primaries.*

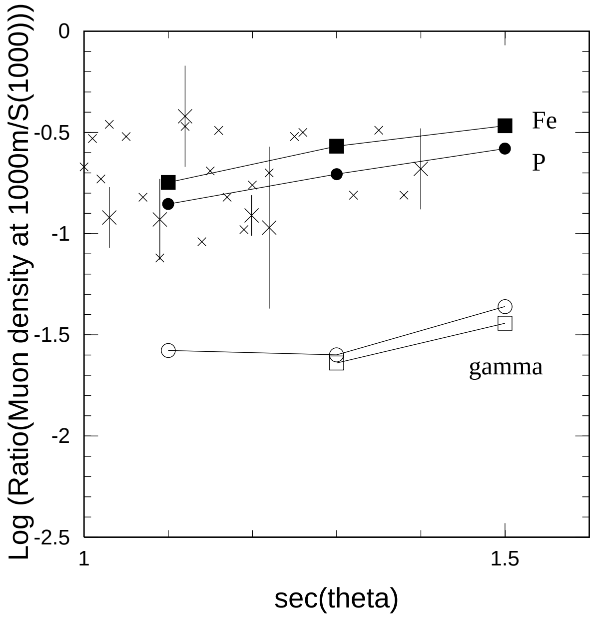

Figure 4: *The relation between observed ρ_μ(1000)/S(1000) and secθ for showers with secθ $\leq$1.4. Results from individual events are shown with crosses for showers $E_0 \geq 10^{19.5}eV$ and large crosses for showers $E_0 \geq 10^{20.0}eV$. Simulation results from CORSIKA for showers of $10^{19.5}eV$ are plotted (closed square:proton, closed square:iron, open circles:gamma-ray (and open squares:gamma-ray of $10^{20}eV$)).*

a factor 1.4 to adjust threshold energy to that of A100. From A1 data, correlation between $\rho_\mu(600)$ and $S(600)$ can be expressed as below and is shown with the broken line in Figure 2.

$$\rho_\mu(600) = 1.4 \times (0.16 \pm 0.01) \quad S(600)^{0.82\pm0.03} \qquad ,(E_\mu \geq 0.5 \times \sec\theta\mathrm{GeV})$$

$\rho_\mu(600)$ increases with $S(600)$ without any significant change of slope up to $E_0 = 10^{19}$eV. The average $\rho_\mu(600)$ for showers with energies greater than $10^{19.0}$eV cannot be determined without a density measurement bias, because of a limited dynamic range of muon density measurement. Instead of $\rho_\mu(600)$, $\rho_\mu(1000)$ is used for the study in the highest energy region. The relation between E_0 and $\rho_\mu(1000)$ is shown in Figure 3. $\rho_\mu(1000)$ of individual air showers with energies greater than $10^{19.5}$eV are also plotted in the same figure. The results from simulation: CORSIKA-QGSJET model, which is developed and provided by Heck et al. (1998), are shown in the same figure for proton, iron and gamma-ray initiated showers with $\sec\theta$ of 1.1 (solid lines). Simulation results for proton and iron showers by Dedenko (private communication) are also drawn in the figure (broken lines). Though there are discrepancies between simulation results in absolute values and slopes, the relation from the experiment seems to be consistent with that from CORSIKA proton simulation. However, the fluctuation of individual points is still too large to get a definite dependence on composition.

In Figure 4, the ratio of observed densities of $\rho_\mu(1000)$ to $S(1000)$ is shown as a function of $\sec\theta$.

Results for individual air showers with energies greater than $10^{19.5}$eV are shown with crosses, and ones for showers with energies $\geq 10^{20.0}$eV are plotted with large crosses. The expected ratios from CORSIKA-QGSJET model for proton, iron and gamma-ray primary showers of $10^{19.5}$eV and for gamma-ray showers of 10^{20}eV are also shown in the same figure. These ratios don't depend on primary energies within simulation uncertainties.

3 Discussions

The energy dependence of the slope of the muon lateral distribution between 800m and 2000m is not observed beyond the experimental uncertainties up to 10^{20}eV as seen in Figure 1.

No indication in the rate of change of the primary composition up to $10^{19.0}$eV has been found from A1 and A100 as discussed in Hayashida et al.(1997). This conclusion is confirmed again by the data acquired up to January 1999 as shown in Figure 2. In the highest energy region above $10^{19.0}$eV, the relation between $\rho_\mu(1000)$ and E_0 has been studied. The slope in the relation seems to be consistent with that expected from CORSIKA proton simulation, but it is much steeper than that from Dedenko simulation. The fluctuation of individual events above $10^{19.5}$eV is too large to infer the change of composition in the highest energy region. We need further experimental study and also simulation study with different models and different simulation codes is also required.

As described in Introduction, it is quite important to examine any gamma-ray primaries in the highest energy region, in order to discriminate the various origin models proposed. It is true that an energy estimation from $S(600)$ is not suitable for gamma-ray primaries. However, since arrival directions of most AGASA $> 10^{20}$eV events are from south and even if they are gamma-ray initiated showers, they are cascaded with a probability of at least 70% in the geomagnetic field (private communication with Vankov,H.P.). Therefore the effect of LPM effect may be relatively small. Also the ratio of $\rho_\mu(1000)$ to $S(1000)$ may not be sensitive to LPM effect, since the number of photoproduced muons depends on the number of photons in a shower. Though the fluctuation of zenith angle dependence of the ratio of $\rho_\mu(1000)$ to $S(1000)$ is large, no candidate of gamma-ray primary is observed, as far as the simulation results of CORSIKA are used, where the LPM effect is taken into account, but not geomagnetic effect. If there are gamma-ray showers of energies above 10^{20}eV and their primary energies are underestimated as below 10^{20}eV but above $10^{19.5}$eV due to LPM effect, they are included in the plots as small crosses in Figure 4. There is again no candidate of gamma-ray shower. We are now estimating photoproduced muons in gamma-ray showers with other simulation codes and details will be reported at the conference.

References

Bird,D.J., Corbato,S.C., Dai,H.Y. *et al., 1993, Proc. 23rd ICRC, Calgary* , **2**, 38

Berezinsky,V.,Kachelriess,M. and Vilenkin,A. *,1997, Phys. Rev. Lett.*, **79**, 4302

Bhattacharjee,P.,Hill,C.T. and Schramm,D.N. *,1992, Phys. Rev. Lett.*, **69**, 567

Chiba,N., Hashimoto,K.,Hayashida,N. *et al., 1992, Nucl. Instr. Meth.*, **A 311**, 338

Hayashida,N., Honda,K., Honda,M. *et al., 1995, J. of Physics G:*, **21**, 1101

Hayashida,N.,Honda,K., Honda,M. *et al., 1997, Proc. 25th ICRC,Durban*, **6**, 241

Heck,D., et al., *,1998, FZKA6019 (Forschungszentrum Karlsruhe, Germany)*

Landau,L.D. and Pomeranchuk,I.J. *,1953, Dokl. Akad. Nauk. SSSR*, **92**, 535

McBreen,B. and Lambert,C.J. *,1981, Phys. Rev. D:*, **24**, 2536

Migdal,A.B. *,1956, Phys. Rev.*, **103**, 1811

Ohoka,H.,Takeda,M.,Hayashida,N. *et al.,1997, Nucl. Instr. Meth.*, **A 385**, 268

Rachen,J.P. and Biermann,P.L., *1993, Astrophys.*, **272**, 161